Chapter IV

Pb(II) Adsorption onto TPVSP and TBVSP

The outcomes of Treated *Pistachio vera* Shell Powder (TPVSP) and Treated Bivalve Shell Powder (TBVSP) as potential sorbents in sequestering Pb(II) from aqueous media are presented in this chapter.

4.1 Microscopic, BET and BJH Analyses

The varied particle sizes of both the treated shells were determined from known mesh sizes using Nikon Diaphot Light Microscope and the respective images for fixed size (0.18 mm) are shown in figures 4.1 (a) and 4.1 (b).

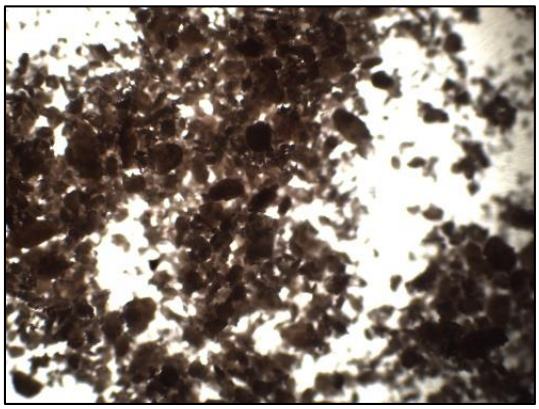

Figure 4.1 (a) TPVSP – Microscopic Image

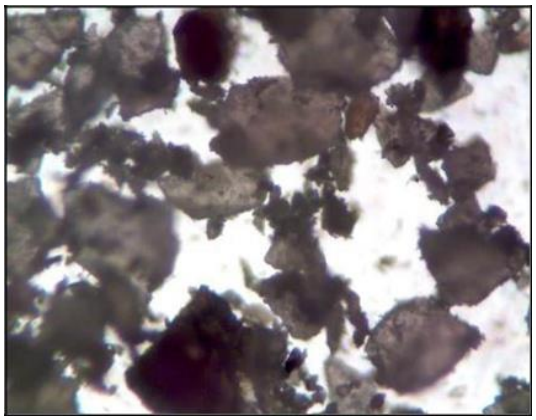

Figure 4.1 (b) TBVSP – Microscopic Image

BET and BJH results revealed the mesoporic nature, in case of both the materials [TPVSP=1.556 nm., TBVSP=24.04 nm], the mean pore diameter values being 199.84 m^2/g and 1.52 m^2/g respectively as evident from figures 4.2 (a), (b) and 4.3 (a), (b). The mesoporous property is indicative of its capability to uptake large sizes of liquid molecules[1].

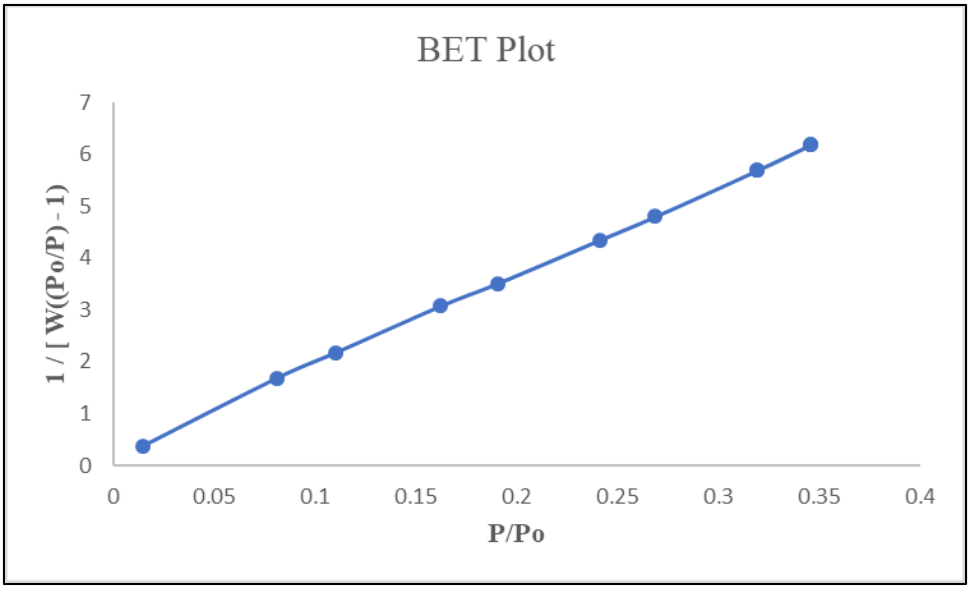

Figure 4.2 (a) BET – TPVSP

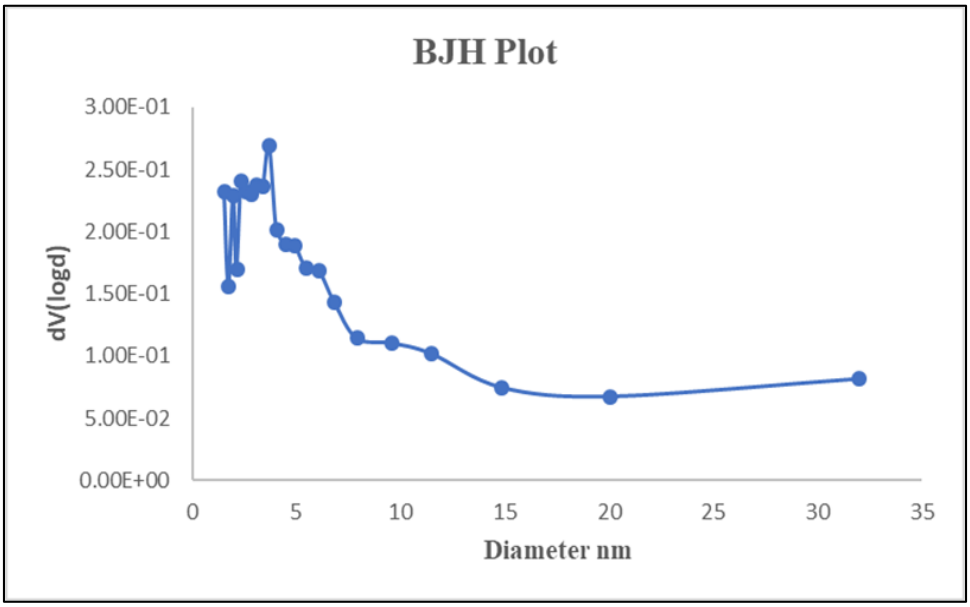

Figure 4.2 (b) BJH - TPVSP

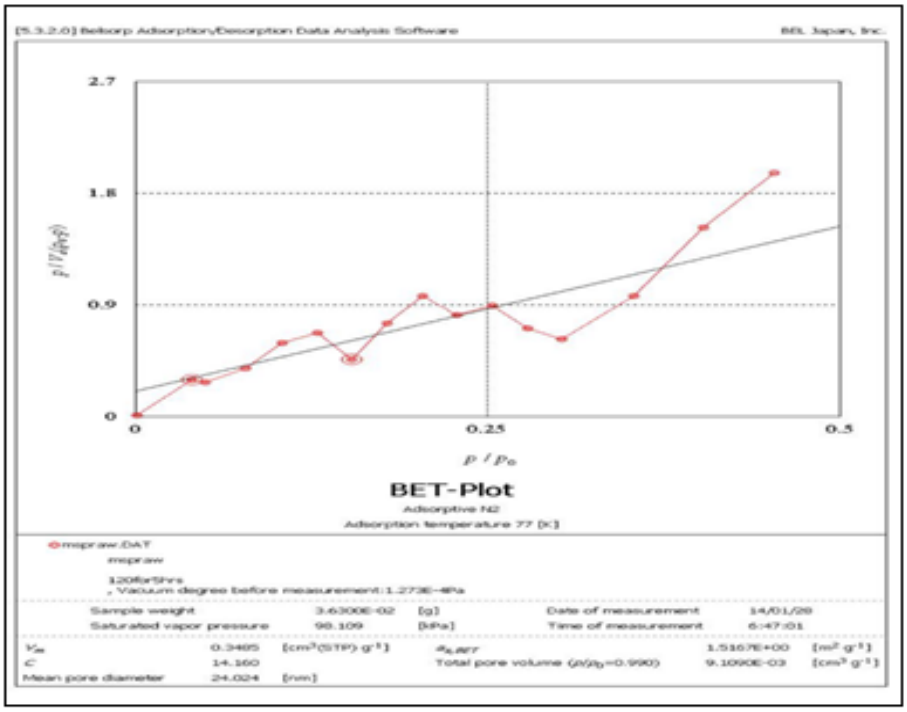

Figure 4.3 (a) BET – TBVSP

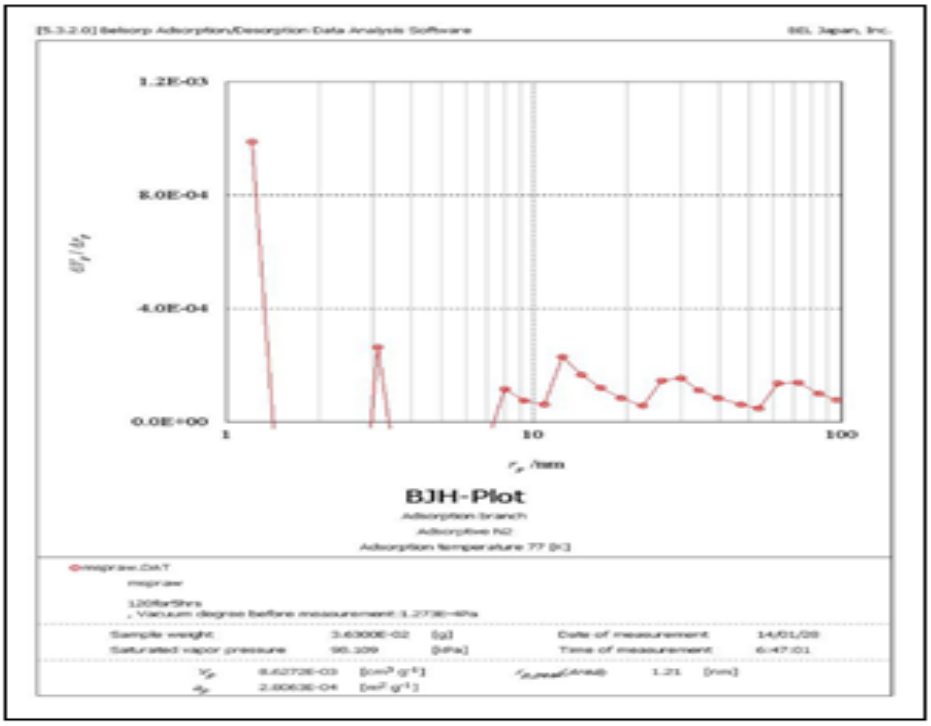

Figure 4.3 (b) BJH - TBVSP

4.2 Physico-Chemical Properties – TPVSP/TBVSP

Table 4.1 lists the parametric values confined to nature/ activity of the modified materials. Lower bulk density values (< 2 g/L) and specific gravities greater than unity support the fine nature of the sorbent particles and less surface tension facilitating better sorption[2]. An approximation of 5% moisture content favour the sorption process[3]. Higher percentage of carbon against the other elements is registered from the CHNS analysis, indicative of lower ash content[4], as it is obvious from the table. Higher pHzpc values (> 7) imply the availability of extended active sites on TPVSP and TBVSP.

4.2.1 Functional Groups Determination

A significant role of functional groups is visualized to study the acid base nature of the sorbents. Carboxylic group forms the major content in preference to phenolic and lactonic groups, promoting negatively charged surface sites due to ionisation of H^+ ions, thereby boosting electrostatic attractive interactions between the negatively charged sorbents' surface and positively charged Pb(II) ions[5].

Table 4.1 Physico-Chemical Parameters

S. No.	Properties	TPVSP	TBVSP
1.	Bulk density (g/L)	0.54	1.67
2.	Specific gravity	1.46	1.86
3.	Porosity	18.56	10.22
4.	Moisture (%)	4.92	5.24
5.	pH (1 % solution)	6.50	10.87
6.	Conductivity	40.16	39.23
7.	Carbon (%)	44.46	43.69
8.	Nitrogen (%)	6.78	2.17
9.	Hydrogen (%)	6.22	5.50
10.	Sulphur (%)	Nil	Nil

S. No.	Properties	TPVSP	TBVSP
11.	Ash content (%)	0.80	4.30
12.	Water soluble matter (%)	1.64	1.89
13.	Acid soluble matter (%)	1.18	1.21
14.	Ion exchange capacity (meq /g)	0.75	0.51
15.	pHzpc	10.08	10.21
16.	Surface area (m^2/g)	199.89	1.51
17.	Mean Pore diameter (nm)	1.55	24.04
Surface Acidic Groups ($mmolg^{-1}$)			
18.	Phenolic	2.39	0.65
19.	Carboxylic	3.65	1.41
20.	Lactonic	2.01	0.29

4.3 Morphological Studies

4.3.1 SEM and EDAX Analyses

The chemical examination of the sorbents was accomplished using energy dispersive X-ray spectrometer (*ZEISS* model) attached to a Scanning Electron Microscope, where direct observations of the surface microstructures pertaining to the bare, treated and Pb(II) laden materials shown in SEM micrographs [figures 4.4(a)-4.5 (c)]. Improvisation in the porous nature is evident from the pictures which establish the increased homogeneity. Also, figures 4.4 (c) and 4.5 (c) portrayed distinguished dark spots relative to Pb(II) adsorption [6].

EDAX spectra [Figures: 4.6 (a) - 4.7(c)] examines the elemental compositions for the three forms of the identified sorbent materials. Chelation of Pb(II) with TPVSP and TBVSP is visible in figures 4.6 (c) and 4.7 (c) through the appearance of peaks at 2.3 Kev.

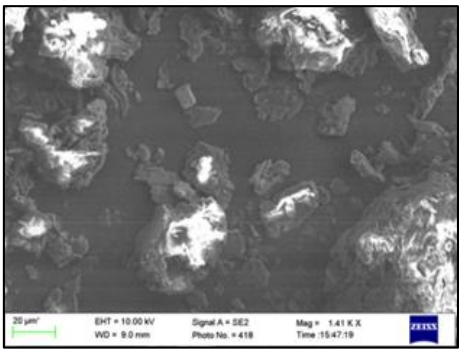

Figure 4.4 (a) SEM - Bare PVSP

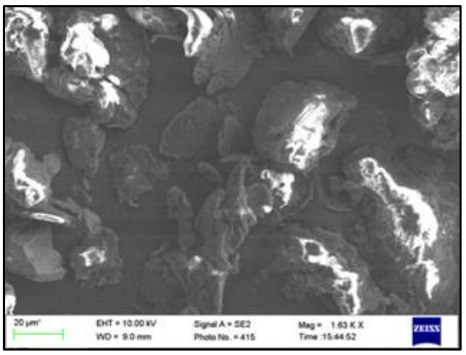

Figure 4.4 (b) SEM - Unloaded TPVSP

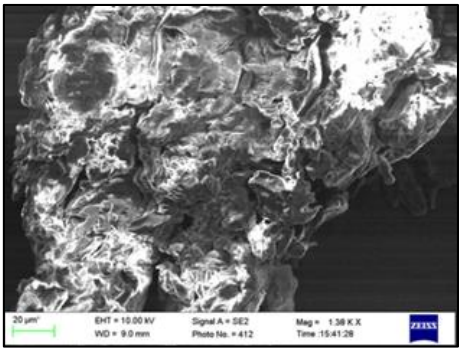

Figure 4.4 (c) SEM - Pb(II)- TPVSP

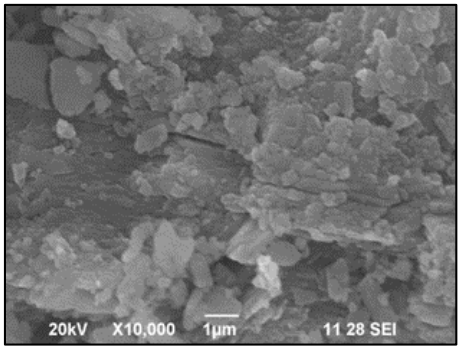

Figures 4.5 (a) SEM -Bare BVSP

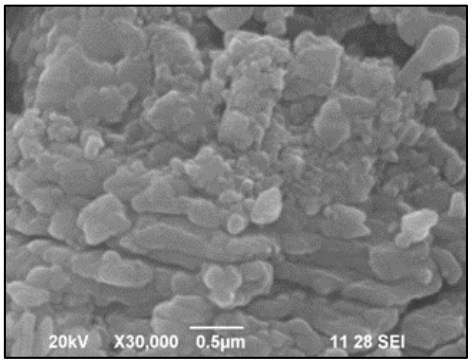

Figure 4.5 (b) SEM - Unloaded TBVSP

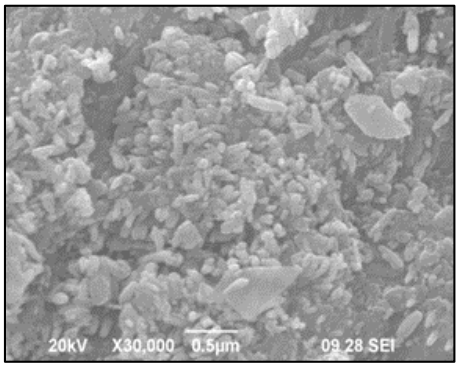

Figure 4.5 (c) SEM -Pb(II)-TBVSP

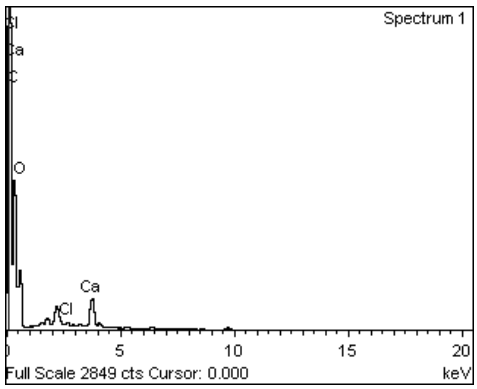

Figure 4.6 (a) EDAX - Bare PVSP

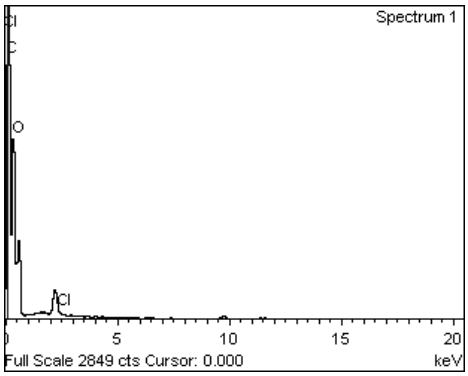

Figure 4.6 (b) EDAX - Unloaded TPVSP

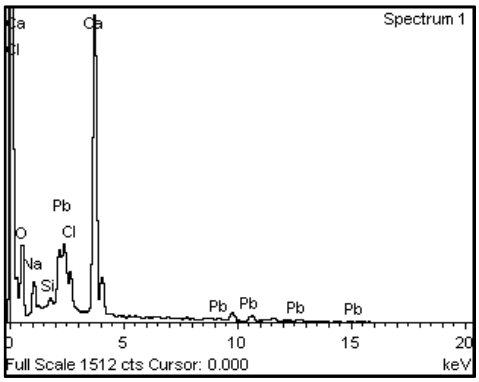

Figure 4.6 (c) EDAX - Pb(II) -TPVSP

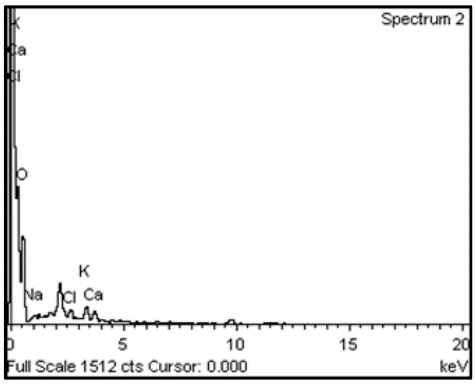

Figure 4.7 (a) EDAX - Bare BVSP

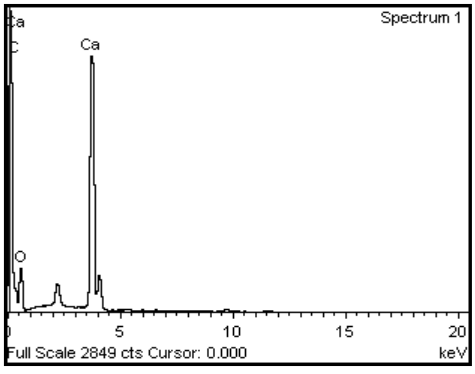

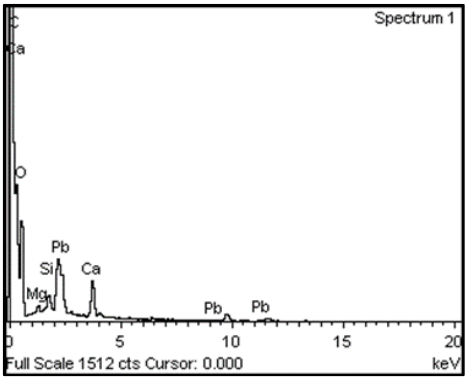

Figure 4.7 (b) EDAX - Unloaded TBVSP Figure 4.7 (c) EDAX - Pb(II) -TBVSP

4.3.2 FTIR Spectral Studies

FTIR spectra of Pb(II) loaded TPVSP and TBVSP along with their counter parts are represented in figures 4.8 (a) - 4.9 (b). Multiple adsorption peaks are scrutinized, evidencing complex nature of the materials. Peaks at 3400cm^{-1}, 2916cm^{-1} ,2852cm^{-1} and 1395 cm^{-1}may be assigned to –OH stretching of hydroxyl group, symmetric and asymmetric C-H stretching vibrations and symmetric bending of CH_3 group[7]. A significant peak shift had occurred from 1700- 1737 cm^{-1}, which can be attributed to the stretching vibrations of carbonyl group in carboxylic acid residues[8]. Similarly, prominent peaks observed within 1350cm^{-1} -1200cm^{-1} band interval shall be ascribed to C-N vibrations[9]. The presence of ionizable functional groups as evidenced from the IR spectra, support the ionization process promoting vacant sites, to be loaded with Pb(II) ions. The disappearance of few peaks in loaded spectra indicate their participation of the metal adsorption process. These changes can be attributed to electrostatic interactions between functional groups of the sorbents and metal cation

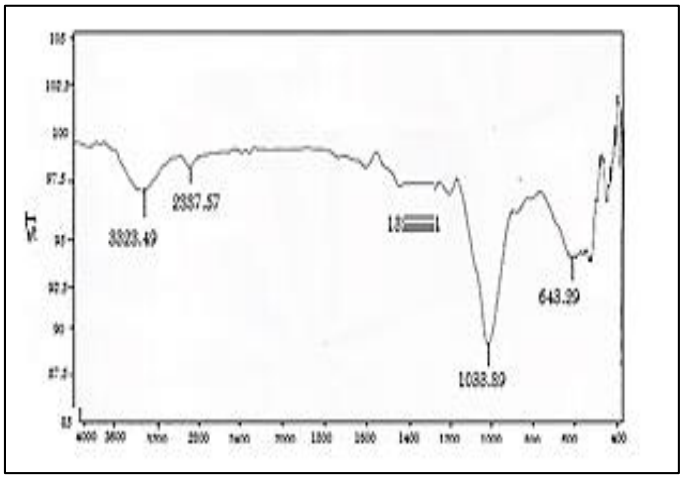

Figure 4.8 (a) FT- IR Unloaded TPVSP

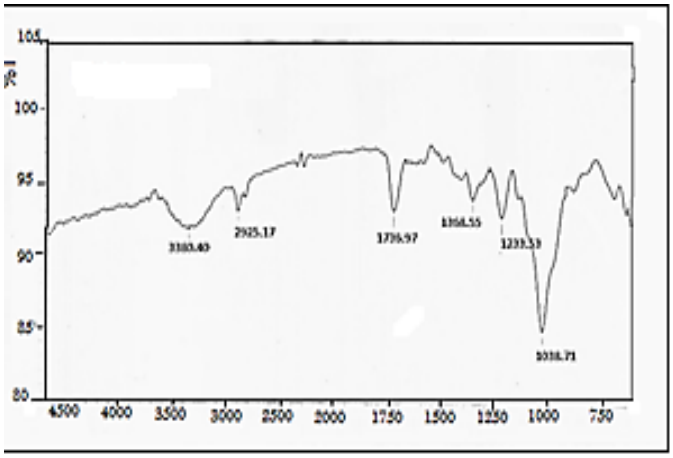

Figure 4.8 (b) FT-IR Pb(II) -TPVSP

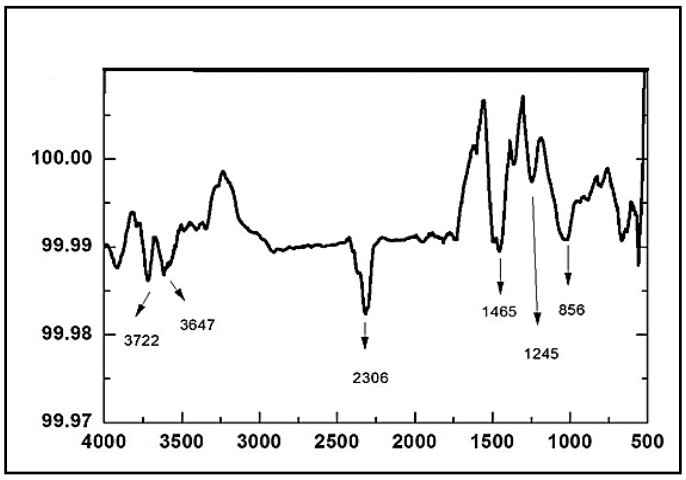

Figure 4.9 (a) FT-IR Unloaded TBVSP

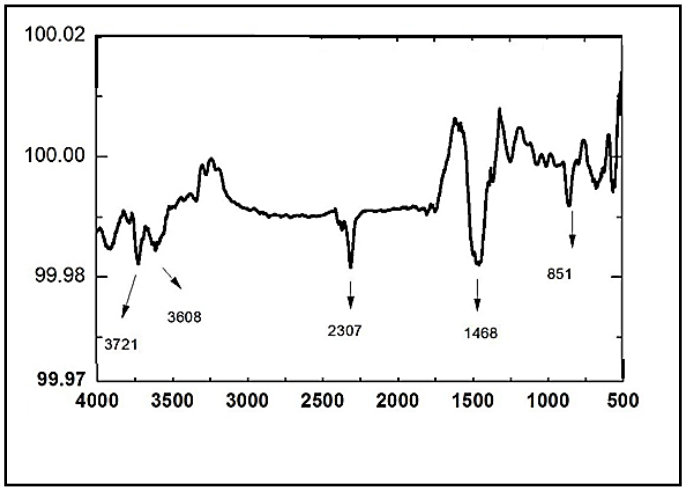

Figure 4.9 (b) FT-IR Pb(II) -TBVSP

4.4 Batch Equilibration Studies

4.4.1 Effect of Particle Size

Figures 4.10 reveals influence of particle sizes (TPVSP and TBVSP: 0.18 mm, 0.24 mm, 0.30 mm, 0.42 mm and 0.71 mm) against the amounts of lead adsorbed. An increasing trend of Pb(II) adsorbed is observed upto 0.18 mm, further reduction in sorption is seen as smooth gradient decline. Thus 0.18 mm, the smaller particle size possessed greater q_e values, substantiating Pb(II) sorption. This is possible due to the larger surface area offering enhanced metal removal for smaller particle size[10].

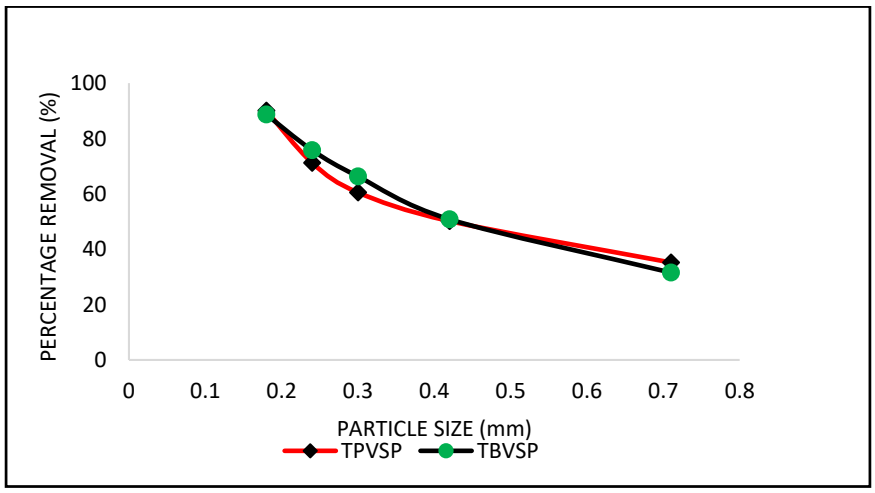

Figure 4.10 Effect of Particle Size

4.4.2 Effect of Initial Concentration and Contact time

The impact of Pb(II) initial concentration and agitation time schemes at preset conditions for TPVSP and TBVSP are depicted in figures 4.11 and 4.12. Figure 4.12 reveals consistent increments in the amounts of Pb(II) adsorbed for 10 mg/L by the display of smooth plateau. Attainment of an equilibrium state is emphasized by the linear nature at 10mg/L Pb(II) concentration up to 10 minutes, could be the reason, suggesting possible monolayer coverage upon TPVSP. Also, reduced amounts of lead adsorbed at concentration higher than 10 mg/L imply the availability of limited sorption sites ratio between sorbent and sorbate species [11]. Thenceforth, a minimum period of 10 minutes and 10 mg/L initial concentration have been chosen as the optimized conditions for

Pb(II)-TPVSP system. However, the rates of amount adsorbed inclined with concentrations as far as TBVSP (Figure 4.12) is concerned, thereby justifying maximum amount adsorbed being exhibited at 25 mg/L. So, 25 mg/L initial Pb(II) concentration was decided as the optimum conditions for TBVSP material.

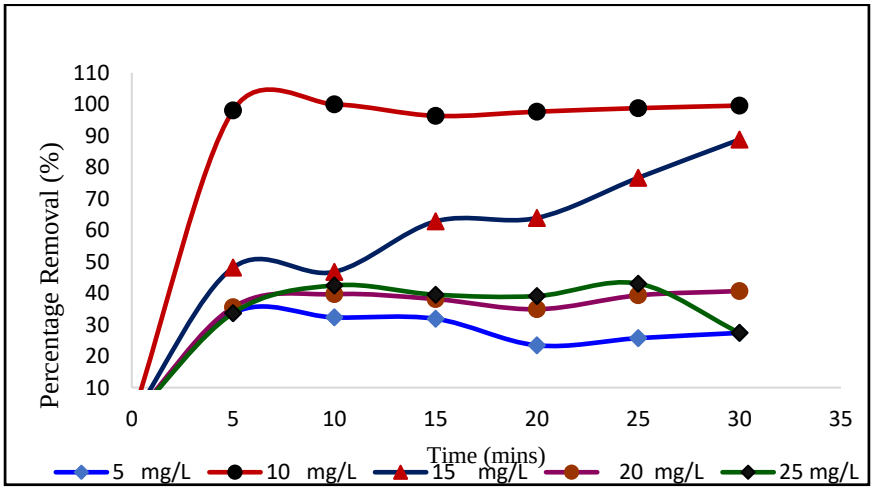

Figure 4.11 Effect of Initial Concentration/ Contact time (TPVSP)

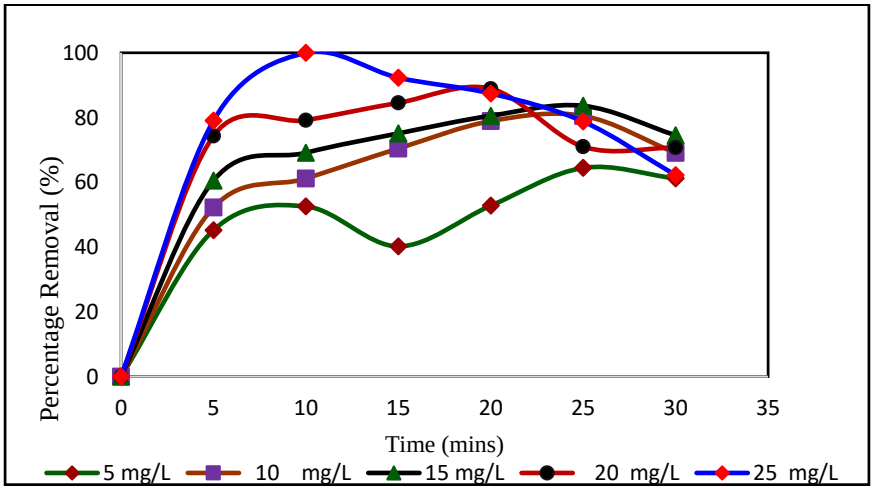

Figure 4.12 Effect of Initial Concentration/ Contact time (TBVSP)

4.4.3 Effect of Dosage

The number of binding sites available for the uptake of sorbate ions depends on the addition of varying doses of sorbents. The influence of dosage disparity (viz., 10 mg, 25 mg, 50 mg, 75 mg & 100 mg) for the two experimented systems are depicted in figures 4.13 and 4.14. A steep inclination was observed in the curves of TPVSP upto 10 mg/L beyond which a saturation point is reached at higher concentrations, where maximized curve is seen for 100 mg dose[12]. However, variation in the curve trends is obvious for TBVSP comparatively inspite of 100 mg to exhibit increased sorption. This irregularity in sorption curves shall be due to overlapping and agglomerating nature of TBVSP. Pb(II) removal at higher dosage reveal the availability of more active.[13]

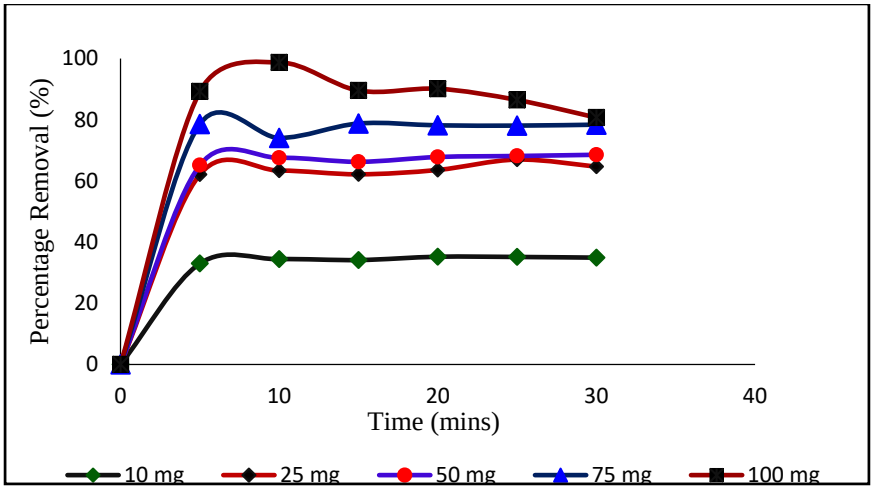

Figure 4.13 Effect of Dosage (TPVSP)

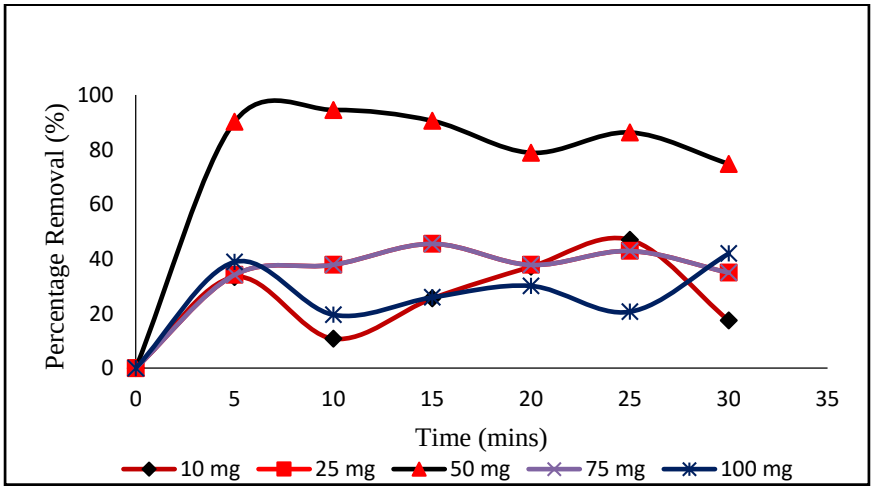

Figure 4.14 Effect of Dosage (TBVSP)

4.4.4 Effect of pH

Approximate parabolic curves for the influence of pH onto TPVSP/ TBVSP systems is depicted in figure 4.15. Maximum percentage removal (97.54 % and 95.26 %) had occurred at pH 5 followed by a dip in the curve. Less sorption at acidic pH show that H^+ ions [14] compete to get adsorbed ahead of Pb(II) ions. Similarly, diminished sorption at alkaline pH support the complex formation of Pb(II) ions with hydroxyl ions [15].

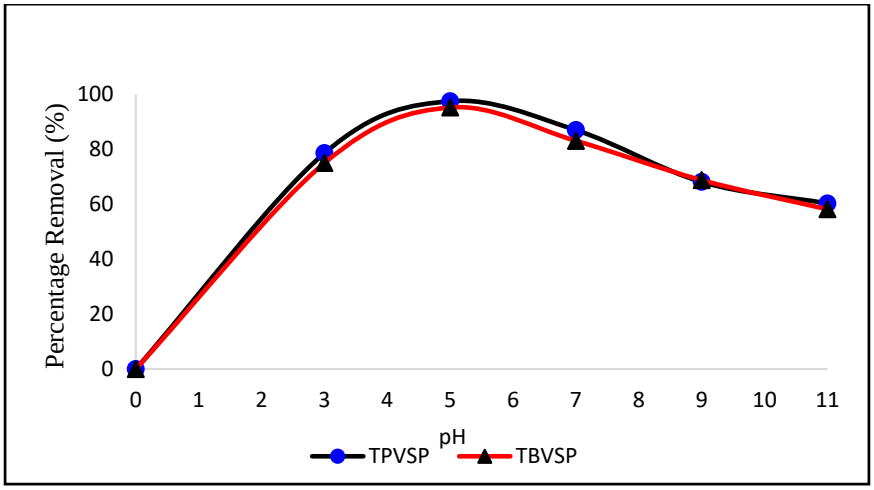

Figure 4.15 Effect of pH

4.4.5 Effect of Cations/ Anions/ Co-ions

Results pertaining to the influence of various cations/ anions/ co-ions are listed in table 4.2. It is evident that, inhibition due to Mg^{2+} was found to be superficial than those of Na^+ in Pb(II) removal. This can be explained in terms of ionic radii [16], where for Mg^{2+} and Na^+, the values are 0.72 Å and 1.02 Å. Smaller the size of cation, greater is its degree of hydration. Therefore, hydrated ionic radii of sodium is greater than magnesium.

Amongst the anions, Cl^- ions exhibited marked inhibition on both the adsorption systems in preference to nitrate ions. This may be due to the facilitation of chloro complex formation of Pb(II) ions, making less availability of Pb(II) ions for sorption process[17]. The co-ionic effects onto Pb(II) system expose Cr^{6+} to inhibit in a greater manner than Zn^{2+}, the reason could be attributed to the fact of Pauling ionic radii, ionization energy and solvation property[18].

Table 4.2 Effect of Cations/ Anions/ Co-ions

Adsorbents	Percentage Removal (%)						
	Pb^{2+} in the	Cations		Anions		Co-ions	
	absence of Ions	Mg^{2+}	Na^{2+}	Cl^-	NO^{3-}	Zn^{2+}	Cr^{6+}
TPVSP	98.7	70.2	89.1	75.7	89.4	86.8	54.2
TBVSP	94.2	66.5	74.3	68.3	85.3	78.1	51.6

4.4.6 Effect of Temperature

The effect of temperature (293-323 K: 10 K) on Pb(II) sorption using TPVSP and TBVSP as per table 4.3 registered a shoot up in the Pb(II) removal at 303K, beyond which an increment is observed at higher temperatures, may be attributed to increase in the flexibility of adsorbate species aiding to a sorption improvisation [19].

Table 4.3 Effect of Temperature

Adsorbents	Percentage Removal (%)			
	293K	303K	313K	323K
TPVSP	65.7	98.7	98.9	99.1
TBVSP	61.4	94.2	95.3	96.6

4.4.7 Desorption/ Regeneration Studies

Desorption studies explores the probability of recycling the loaded adsorbents and regenerating the same for further sorption process. Studies were carried out for Pb(II) TPVSP/ TBVSP systems to assess the efficiencies of the packed sorbents by employing various strengths of HCl. The percentage of desorption was inversely proportional to HCl [20] strength (Figure 4.16) Also, desorption percentage was observed to be higher for TPVSP than TBVSP, thereby establishing better regeneration efficiency of the latter, as evident from the two successive desorption and regeneration cycles (Figures 4.17 and 4.18).

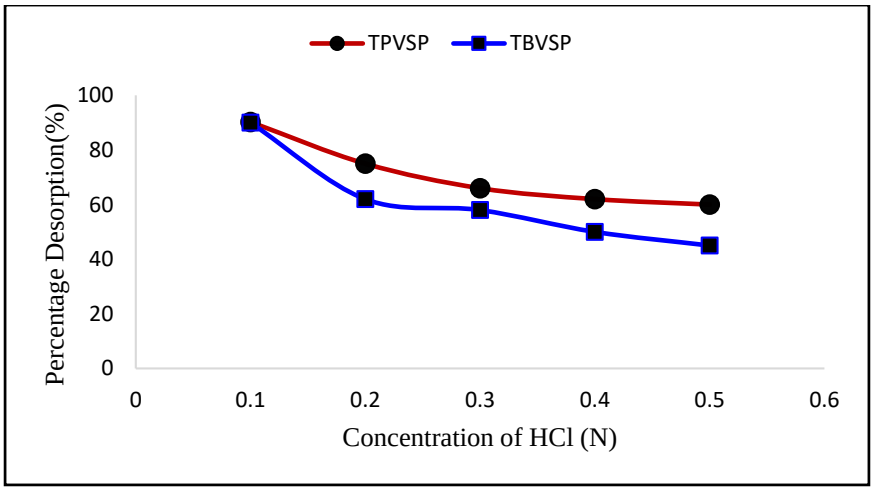

Figure 4.16 Desorption of Pb(II)

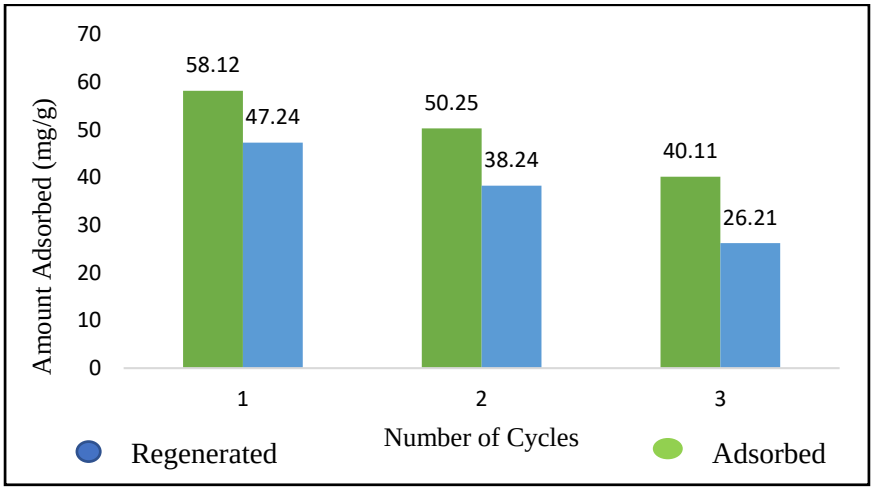

Figure 4.17 Pb(II) -TPVSP - Regeneration

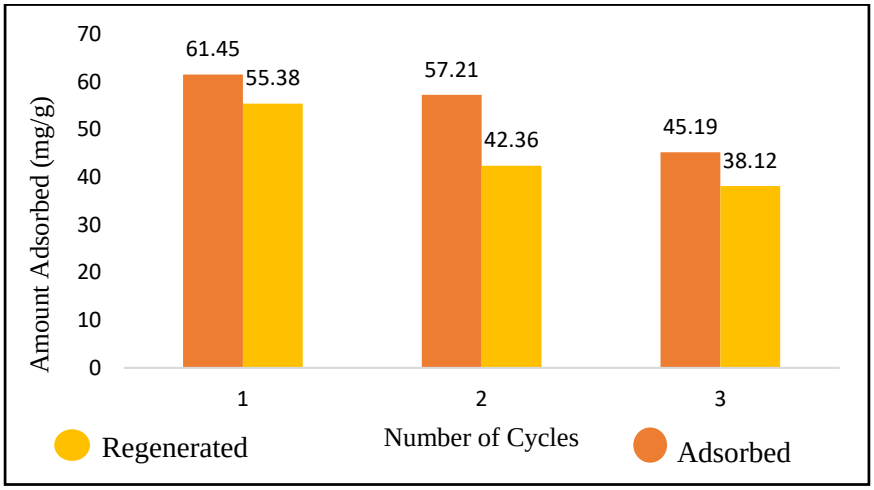

Figure 4.18 Pb(II) -TBVSP - Regeneration

4.5 Isothermal Studies

Adsorption isotherm is a key factor to determine the adsorption process. Different adsorption isotherm models viz., Langmuir, Freundlich and DKR have been deliberated for the two verified systems.

4.5.1 Langmuir Model

The equilibrium concentrations of Pb(II) and adsorption capacities of TPVSP/ TBVSP for the confiscation of the former, derived from experimental data are utilized to depict Langmuir plots, (Figures 4.19 and 4.20) whose corresponding data are represented in table 4.4. The linear fit of the plots is supported by the correlation coefficient values (nearness to unity) as mentioned in the graph. The isothermal constants (q_m,b) corresponding to sorption capacities and intensities calculated from the plots and separation factor, R_L (referred in 3.16.1) are listed in table 4.6. Lower 'b' values (<4) favor the sorption system to obey Langmuir model, with monolayer coverage.

Table 4.4 Equilibrium Concentrations'-Isothermal Data

Systems	Metal Ion Conc. (mg/L)	Langmuir		Freundlich		DKR	
		C_e	C_e/q_e	log C_e	log q_e	$\grave{\varepsilon}^2*10^{-5}$	ln q_e
Pb(II) - TPVSP	5	4.77	0.08	0.68	1.79	2.30	4.11
	10	8.98	0.13	0.95	1.84	0.71	4.23
	15	13.65	0.18	1.14	1.87	0.32	4.31
	20	19.48	0.28	1.29	1.90	0.16	4.26
	25	24.98	0.40	1.40	1.96	0.10	4.13
Pb(II) - TBVSP	5	4.78	0.14	0.68	1.89	2.29	3.51
	10	8.91	0.14	0.95	1.85	0.72	4.15
	15	13.52	0.26	1.13	1.62	0.32	3.95
	20	19.85	0.52	1.30	1.54	0.15	3.63
	25	24.89	0.67	1.40	1.42	0.10	3.62

Table 4.5 Isothermal Constants

Systems	Langmuir			Freundlich			DKR		
	q_m (mg/g)	b (L/g)	R^2	K_F (mg/g)	1/n	R^2	q_s (mg/g)	E (KJ/mol)	R^2
Pb(II) – TPVSP	63.69	1.33	0.9789	42.58	0.22	0.9530	69.79	3.14	0.3004
Pb(II) - TBVSP	35.21	0.45	0.9456	252.46	0.67	0.9206	46.58	2.30	0.1034

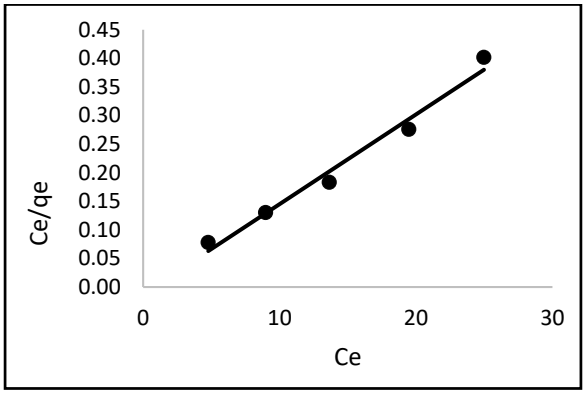

Figure 4.19 Langmuir Plot (TPVSP)

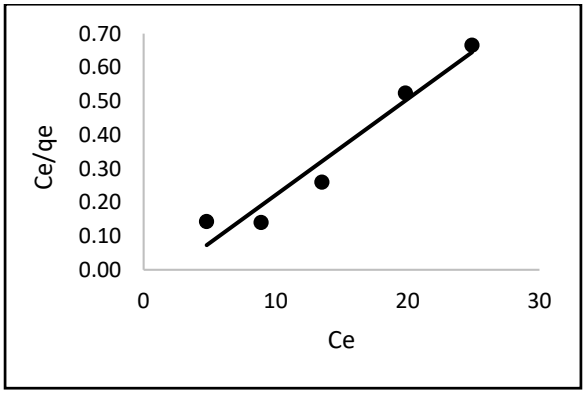

Figure 4.20 Langmuir Plot (TBVSP)

Table 4.6 Equilibrium Parameter (R_L)

Conc. (mg/L)	Pb(II)-TPVSP	Pb(II)-TBVSP
5	0.13	0.31
10	0.07	0.18
15	0.05	0.13
20	0.04	0.10
25	0.03	0.08

4.5.2 Freundlich Model

A plot between log q_e vs log C_e is shown in figures 4.21 and 4.22, where the logarithmic values are found to lie in a straight line with a correlation coefficient in the range of 0.9, indicative of the better fit of the model to the systems. The isothermal constant 1/n as evident from table 4.5 lie in the range of 0 - 0.1, favoring[22] the acceptability of Freundlich model also. However, from the recorded observations it is understood that, the preferable model is Langmuir for both the systems.

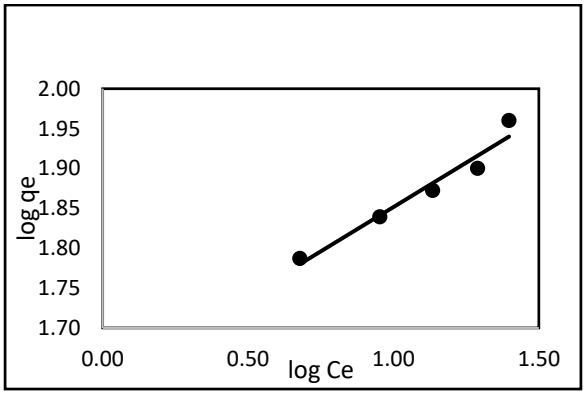

Figure 4.21 Freundlich Plot (TPVSP)

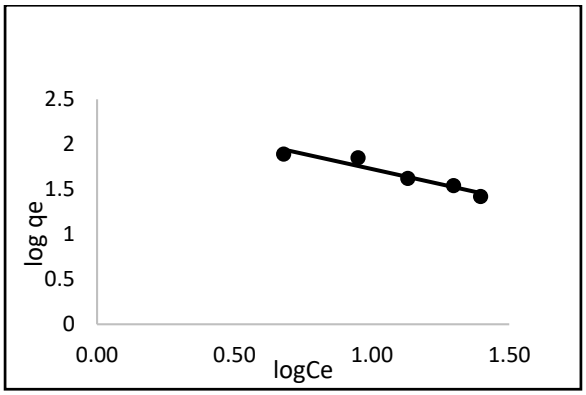

Figure 4.22 Freundlich Plot (TBVSP)

4.5.3 Dubinin–Kaganer-Radushkevich Model (DKR)

E values of DKR isotherms being 3.14 and 2.30 KJ/mol^{-1} for Pb(II)-TPVSP and Pb(II)-TBVSP systems are apparent from table 4.5. The role of weak Vander Waals forces i.e., E< 8 KJ/mol^{-1} endure physisorption inlieu with the exemplified data, where physisorption[26] is ascribed as the operating factor for the uptake of divalent ions by both the adsorbents.

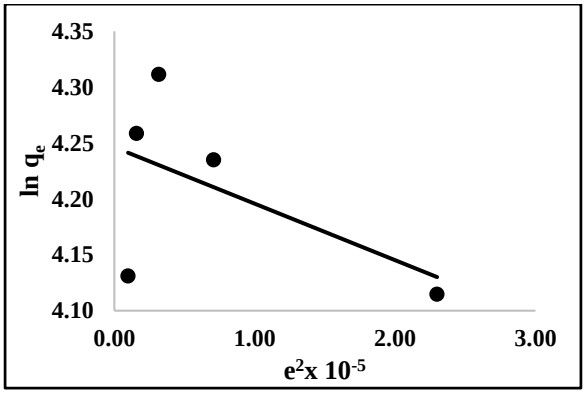

Figure 4.23 DKR Plot (TPVSP)

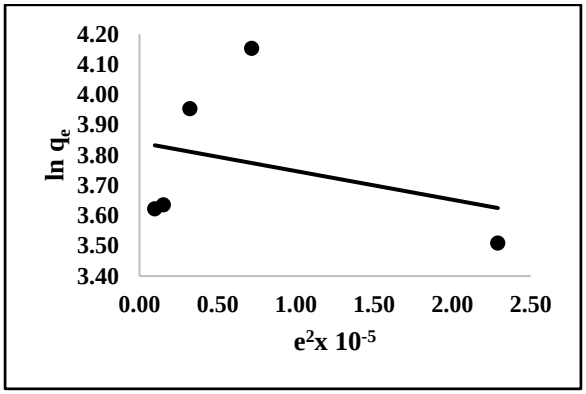

Figure 4.24 DKR Plot (TBVSP)

4.5.5 Isotherms- A Comparison

Among all isotherms described, Langmuir model is preferred by the systems emphasizing monolayer adsorption onto the homogeneous surfaces of TPVSP and TBVSP. Favorability of physisorption is confirmed by the lesser 1/n values, wherein, multilayer adsorption is less determined. DKR constants' values derived from the respective plots is

in favor of physisorption in alignment with Langmuir model. Thence, the applicability of the models is ordered as Langmuir> Freundlich> DKR. This statement is in good agreement with the results registered by S A Bhalerao et al., [27].

4.6 Adsorption Dynamics

Thermodynamic factors ΔH^o and ΔS^o (Table 4.7), determined by the slopes and intercepts of the Van't Hoff's plots (Figures 4.25 and 4.26) derived as per equation 13 (chapter III-3.18) show positive values. The change in enthalpy (ΔG^o) is calculated from ΔH^o and ΔS^o. The positivity of enthalpy/ entropy variations and the negativity of enthalpy variation promote the endothermicity[28,29], prominent degree of disorderliness and feasibility of the reactions. These observed changes at the solute- solution interface may be attributed to the fact that, the adsorbed water molecules, which are displaced by the adsorbate species, gain more translational entropy than is lost by the adsorbate molecules, thus allowing the prevalence of randomness in the system[30].

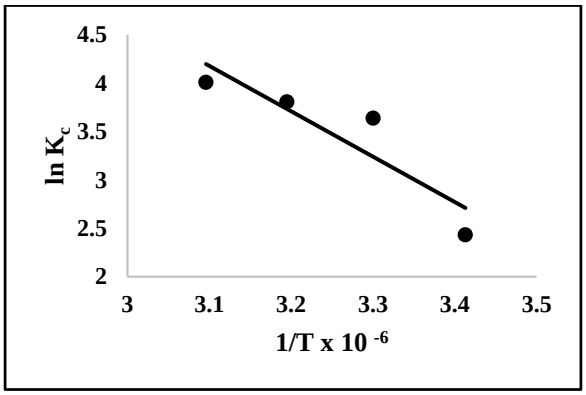

Figure 4.25 Van't Hoff's Plot (TPVSP)

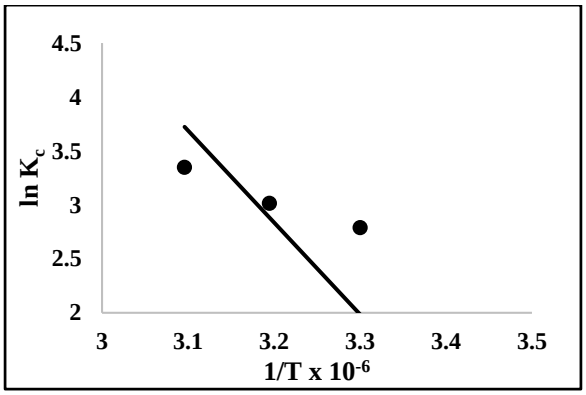

Figure 4.26 Van't Hoff's Plot (TBVSP)

Table 4.7 Thermodynamic Parameters

Temp. (K)	Pb(II) - TPVSP			Pb(II) – TBVSP		
	$\Delta G°X\ 10^{-3}$ (kJ/mol)	$\Delta H°$ (kJ/mol)	$\Delta S°$ (J/mol K)	$\Delta G°X\ 10^{-3}$ (kJ/mol)	$\Delta H°$ (kJ/mol)	$\Delta S°$ (J/mol K)
293	-0.11	4.69	18.73	-0.12	8.51	30.09
303	-0.92			-0.70		
313	-0.99			-0.78		
323	-1.08			-0.90		

4.7 Conclusion

Sorptive behavior of *Pistachio vera* shells and Bivalve shells powder (PVSP/ BVSP) in the removal of Pb(II) ions, from aqueous media , after chemical modifications is described in chapter IV. The chosen materials were pulverized, categorized into varying particle sizes before subjecting them to modification. Characterization studies viz., microscopic, BET/ BJH, physico-chemical parameters, SEM, EDAX and FT-IR for the prepared materials (TPVSP/ TBVSP) and the surface changes of Pb(II) loaded counterparts were carried out after conducting Batch experimental verification. Batch mode studies comprised of optimizing variable factors, to determine the best conditions in case of both Pb(II)- TPVSP and Pb(II)-TBVSP systems. Fixed values for the maximum Pb(II) removal were established as, 0.18 mm particle size, 100 mg/ 10 mg/L and 50 mg/ 25 mg/L of doses/ initial concentrations for TPVSP and TBVSP, 10 minutes agitation time, pH 7 and 30ºC room temperature. Cationic/ anionic influence upon the studied systems proved that marked inhibition is exhibited by cations in preference to anions. Desorption of the exhausted materials followed by regeneration studies were carried out to ensure the economic value of the adsorption processes. Nature of adsorption was established by isothermal and thermodynamic factors, wherein, the applicability of Langmuir model suggested monolayer adsorption. Negative $\Delta G°$ and positive $\Delta H°$/ $\Delta S°$ values favored the systems to be feasible, endothermic and greater randomness respectively. Even though, approximately 98% Pb(II) removal (10 mg/L) was registered for 100 mg of TPVSP; TBVSP had shown 94% for 25 m/L initial Pb(II) concentration at half dose itself, emphasizing its better sorption characteristics

4.8 References

1. A.S. Sartape, P. D. Raut, Efficient Adsorption of Cr (VI) from Aqueous Solution on Low Cost Adsorbent Developed from *Limonia Acidissima* (Wood apple) Shell, *Advance Science & Technology*, 28(6), (**2010)**, 547-560.

2. V.C. Srivastava, I. D. Mall and I. M. Mishra, Characterization of Mesoporous Rice Husk Ash (RHA) and Adsorption Kinetics of Metal Ions from Aqueous Solution onto RHA, *Journal of Hazardous Materials*, 134, (**2006**), 257-267.

3. V.P Della, I. Kuhn and D. Hotza, Characterization of Rice Husk Ash for use as Feedstock in the Manufacture of Silica Refractories, *Quimica Nova*, 24, (**2008**), 778-782.

4. E. Demirbas, M. Kobya, A. E. S. Konukman, Error Analysis of Equilibrium Studies for the Almond Shell Activated Carbon Adsorption of Cr(VI) from Aqueous Solutions, *Journal of Hazardous Materials*, 154, (**2008**), 787-794.

5. S. L Goertzen, K. D Thériault, A. M Oickle, A.C Tarasuk, and H.A Andreas, Standardization of the Boehm Titration-PartI: CO2 Expulsion and Endpoint Determination, *Carbon*, 48(4), (**2010**), 1252–1261.

6. Parlayici, S. Pehlivan, Natural Biosorbents (garlic stem and horse chesnut shell) for Removal of Chromium (VI) from Aqueous Solutions, *Environmental Monitoring and Assessment*, 187(12), (**2015**), 763.

7. A. Dandekar, R T K.Baker, M A Vannice, Characterization of Activated Carbon, Graphitized Carbon Fibers and Synthetic Diamond Powder using TPD and DRIFTS, *Carbon*, 36, (**1998**), 1821-1831.

8. Gurdeep Chatwal, K.Sham Anand, Instrumental Methods of Chemical Analysis, 5th Edition, *Himalaya Publishing House*, New Delhi, India (**2007**).

9. Mehrasbi, M R Farahmandkia, Z Taghibeigloo, B Taromi, Adsorption of Lead and Cadmium from aqueous Solutions by using Almond Shells, Water, Air, Soil Pollution, 199,(**2009**), 343–351.

10. Michael Horsfall, Jnr and L. Jöse Vicente, Kinetic Study of Liquid-Phase Adsorptive Removal Of Heavy Metal Ions By Almond Tree (*Terminalia Catappa L*.) Leaves Waste, *Bulletin Journal of Chemical Society Ethiopia,* 21(3), (**2007**), 349-362.

11. Muhammad Riaz, Raziya Nadeem, Muhammad AsifHanif, Tariq Mehmood Ansari, Khalil-ur-Rehman, Pb(II) Biosorption from Hazardous Aqueous Streams using *Gossypium Hirsutum* (Cotton) waste Biomass, *Journal of Hazardous Materials,* 161, (**2008**), 88-94.

12. S. Rengaraj, Kyeong-Ho Yeon, So-Young Kang, Jong-Un Lee, Kyung-Woong Kim, Seung-Hyeon Moon, Studies on Adsorptive Removal of Co(II), Cr(III) and Ni(II) by IRN 77 Cation-Exchange Resin, *Journal of Hazardous Material,* 92, (**2002**), 185-198.

13. J. AnandKumar, B. Mandal, Removal of Cr(VI) from Aqueous Solution using Bael Fruit (*Aegle marmeloscorrea*) Shell as an Adsorbent, *Journal of Hazardous Materials,* 168, (**2009**), 633-640.

14. Mohammed Ajmal, Rifaquat Ali Khan Rao, Rais Ahmad, Jameel Ahmad, Adsorption Studies on Citrus Reticulate Removal and Recovery of Ni(II) from Electroplating Waste Water, *Journal of Hazardous Material*, 79, (**2005**), 117-131.

15. R. Ayyappan, A. Carmalin Sophia, K. Swaminathan, S. Sandhya, Removal of Pb(II) from Aqueous Solution using Carbon Derived from Agricultural Wastes, *Process of Biochemistry.* 40, (**2005**), 1293-1299.

16. P. L. Soni, Mohan Katyal, Text Book of Inorganic Chemistry (Modern Approach), Sultan Chand & Sons, 20th Revised edition, *Educational Publishers,* New Delhi, India (**2001**).

17. Tarun Kumar Naiya, Ashim Kumar Bhattacharya, Sailendranath Mandal, Sudip Kumar Das, The Sorption of Lead(II) Ions on Rice Husk Ash, *Journal of Hazardous Materials,* 163, (**2009**), 1254-1264.

18. N. Muthulakshmi Andal, Studies on the Adsorption of Iron(III), Copper(II), Zinc(II) and Chromium (VI) using Naturally Occurring Polymers -Ph.D Thesis, Gandhigram Rural University , Gandhigram, Dindigul, Tamil Nadu, India.

19. Aik Chong Lua, Ting Yang, Virtual Screening of Treated *Pistachio vera* Shell Powder as a Potential Sorbent in Sequestering Ubiquitous Divalent Metal Ions from Aqueous Matrices, *Journal of Colloid Interface and Science*, 274, (**2004**), 594–60.

20. G.S Agarwal, Hitendra Kumar Bhuptawat, Sanjeev Chaudhari, Biosorption of Aqueous Cr(VI) by *Tamarindus indica* Seeds, *Bioresource and Technology*, 97, (**2006**), 949-956.

21. T. S. Anirudhan and M. K. Sreedhar**,** Modified Coconut Husk for Mercury Removal from Wastewater, *Pollution Research*, 17(4), **(1998),** 381 – 384

22. C. K. Singh, J. N. Sahu, K. K. Mahalik, C.R. Mohanty, B. Raj Mohan, B.C.Meikap, Studies on the Removal of Pb(II) from Wastewater by Activated Carbon Developed from Tamarind Wood Activated with Sulphuric Acid, *Journal of Hazardous Materials*, 153, (**2008**), 221-228.

23. G. Vazquez, J. Gonzalez-Alvarez, S. Freire, M. Lopez-Lorenzo, G. Antorrena, Removal of Cadmium and Mercury Ions from Aqueous Solution by Sorption on Treated Pinus Pinaster Bark: Kinetics and Isotherms, *Bioresource and Technology*, 82, (**2002**), 247-251.

24. Hakan Demiral, Ilknur Demiral, Fatma Tumsek, Belgin Karabacakoglu, Adsorption of Cr(VI) from Aqueous Solution by Activated Carbon Derived from Olive Bagasse and Applicability of Different Adsorption Models, *Chemical Engineering Journal*, 144, (**2008**), 188-196.

25. A.O. Olalekan, A. P ,Olatunya, A.M. Dada, Langmuir, Freundlich, Temkin and Dubinin–Radushkevich Isotherms Studies of Equilibrium Sorption of Zn^{2+} Unto Phosphoric Acid Modified Rice Husk Dada, *Journal of Applied Chemistry,* 3(1), (**2012**), 38-45.

26. C. Daniel Emeniru, D. OkechukwuOnukwuli, Pere-ere DouyeWodu, I. Bernard Okoro The Equilibrium and Thermodynamics of Methylene Blue Uptake onto Ekowe Clay; Influence of Acid Activation and Calcination, *International Journal of Engineering and Applied Sciences*, 2(5), (**2015**), 17-25.

27. A. Satish Bhaleraoa, C. Anukthi Poojaria and D. Sandip Maindb, Biosorption Studies of Cadmium (ii) Ions from Aqueous Solutions onto Orange Rind (*Citrus Sinensis l. osbeck*), *Octa Journal of Environmental Research International,* 3(1), (**2015**), 028-040.

28. Emine Malkoc, Yasar Nuhoglu, Determination of Kinetic and Equilibrium Parameters of the Batch Adsorption of Cr(VI) onto Waste Acorn of *Quercus ithaburensis, Chemical Engineering and Processing,* 46, (**2007**), 1020-1029.

29. B. Stephan Inbaraj and N. Sulochana, Basic Dye Adsorption on a Low Cost Carbonaceous Sorbent - Kinetic and Equilibrium Studies, *Journal of Chemical and Technology*, 9, (**2002),** 201 – 208

30. Ting Fan, Yunguo Liu, Baoying Feng, Guangming Zeng, Chunping Yang, Ming Zhou, Haizhou Zhou, Zhenfeng Tan, Xin Wang, Biosorption of Cadmium(II), Zinc(II) and Lead(II) by *Penicillium Simplicissimum:* Isotherms, Kinetics and Thermodynamics, *Journal of Hazardous Materials*, 160 (**2008**), 655-661.